Organic molecular solids as thin film transistor semiconductors

H. E. Katz

Bell Laboratories, Lucent Technologies, 600 Mountain Avenue, Murray Hill, NJ 07974, USA

The use of discrete organic compounds as active materials in transistors is described, beginning with α-sexithiophene (α-6T) and progressing to other thiophene oligomers and nonthiophene semiconductors. Device operation, molecular design, synthesis, film morphology and transport of holes and electrons are covered.

Thin film transistors (TFTs) based on organic semiconductors are envisioned as key components of plastic circuitry for use as display drivers[1] in portable computers and pagers, and as memory elements in transaction cards and identification tags.[2] Such transistors are by no means expected to replace silicon in high performance or high density devices, but instead are aimed at applications where ease of fabrication, mechanical flexibility and avoidance of high temperature excursions are of particular importance. Organic TFTs are just one class of organic devices, of which rectifiers, light-emitting diodes, photodetectors, solar cells, electro-optic switches and sensors are other representative examples.[1,3] Since each of these latter devices would merit extensive discussion in their own right if treated here, they will instead be considered to be outside the scope of the present discussion, which will be devoted exclusively to materials issues relevant to the development of organic TFTs.

A generic embodiment of a TFT device is shown in Fig. 1.[3] The 'off' state is defined as the case of little or no current flowing between the source and drain electrodes at a given source–drain voltage, while the 'on' state refers to the case where substantial source–drain current flows at that voltage. Switching between the two states is accomplished by the application and removal of an electric field from the gate electrode across the gate dielectric to the semiconductor–dielectric interface, effectively charging a capacitor. When the TFT operates in the so-called accumulation mode, the charges on the semiconductor side of the capacitor, injected from the source, are mobile and conduct the source–drain 'channel' current. For 'p-type' semiconductors, where the organic molecules would be considered electron donors, the carriers are holes, while electron-accepting organics are 'n-type' and form channels of electrons. In the absence of a gate field, there is no channel and ideally no source–drain conduction. In practice, however, there can be adventitious off-currents caused by impurities in the semiconductor and by leakage pathways.

While the device structure is fairly specifically defined, there is some possible variability. The source and drain electrodes can be fashioned directly on the gate dielectric as in Fig. 1, in an arrangement known as 'bottom contacts', or alternatively, on top of the semiconductor, the so-called 'top contact' geometry of Fig. 2. In the former arrangement, charge need only be injected laterally from the source to form the channel, while the latter alternative requires perpendicular charge transport as well. This could be aided by selective doping of the semiconductor under the contacts.[4] The top contact geometry has the advantage of larger and more intimate metal–semiconductor charge transfer interfaces than does the bottom contact geometry.[4] As will be discussed below, the active material can comprise two or more semiconductors, varying in bandgap, band energy, or type, either mixed or in separate layers. The metal and dielectrics can be composed of a variety of materials as well.[4] Finally, the TFTs can be assembled and cascaded to form higher-order circuit elements.

The semiconductor must possess several distinct but interrelated attributes. The material must accept charge without a substantial barrier from the source electrode. The charge must migrate quickly between the source and the channel without large hysteresis. The mobility must be high enough to allow useful quantities of source–drain current to flow, modulated by accessible voltage and power. The semiconductor and other materials with which it is in contact must withstand the operating conditions without thermal, electrochemical or photochemical degradation. These requirements define the necessary band levels, bandgaps and surface states for the semiconductors to perform, as illustrated in Fig. 3. Again, at a 'reasonable voltage', the highest occupied and lowest unoccupied molecular orbitals (analogous to valence and conduction band energy levels in inorganic semiconductors) must be altered so that holes or electrons will enter the channel region as needed, without creating chemical instability.[5] Too high a bandgap would probably mean that the bands themselves would be too far in energy from the voltage-modified charge carrier energies at the semiconductor interfaces. For a given level of chemical or morphological defects, the probability of trap states would also increase in high bandgap materials. However, too low a bandgap or low charge carrier energies increase the likelihood of thermal excitation or chemical doping of the materials, making them difficult to turn 'off'. The

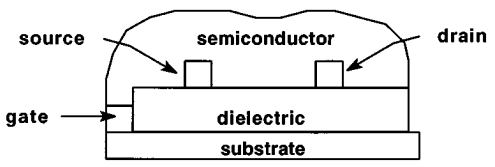

Fig. 1 Schematic structure of an organic TFT, with the usual 'bottom contact' geometry. The substrate is conductive and often consists of heavily doped Si. The dielectric would then be SiO_2. The source, drain and gate contacts are typically gold, but other metals or conductive composites can be used.

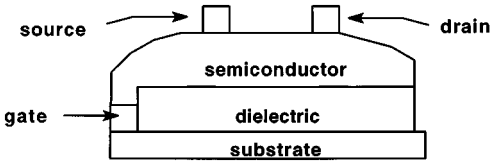

Fig. 2 TFT structure illustrating the 'top contact' geometry

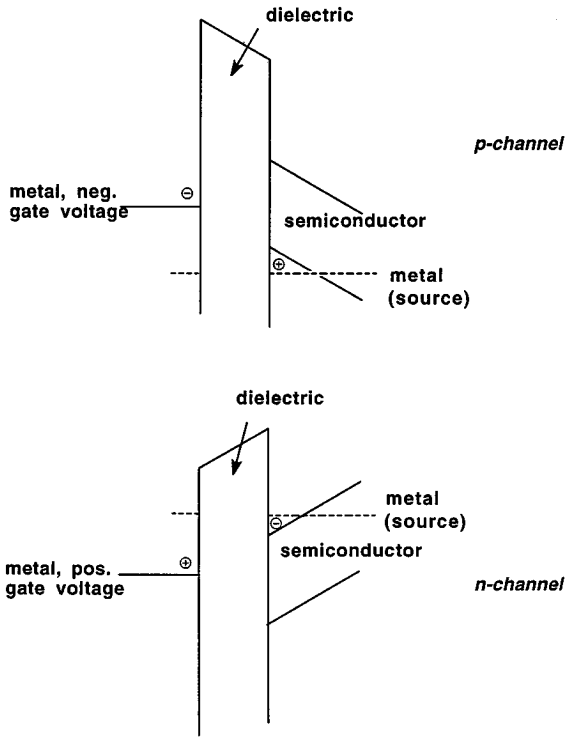

Fig. 3 Relative electronic energy levels of TFT components, under hole-injection (p-channel) and electron-injection (n-channel) conditions

surfaces of the metal contacts and the surface functionality of the dielectric affect these performance characteristics by influencing the interfacial charge carrier energies, determining the local solid state structure of the semiconductor and acting as sites of unwanted traps and chemical reactions.

The two performance parameters that must be optimized in TFTs are field effect mobility (μ_{FE}) and on/off ratio. The former is related to the absolute quantity of 'on' current (I_{on}) that can be induced in the device, and is defined for the regimes where current is linear with respect to source–drain voltage, and 'saturated' (independent of source–drain voltage) in eqn. (1) and (2), respectively,

$$I_{on} = [WC_i\mu_{FE}\ V_D(V_G - V_O)]/L \quad (1)$$

$$I_{on} = [WC_i\mu_{FE}\ (V_G - V_O)^2]/2L \quad (2)$$

where W and L are channel width and length, respectively, C_i is the capacitance per unit area of the gate dielectric, and V_D, V_G and V_O are the drain–source, gate–source and threshold voltages, respectively.

The latter expresses this current relative to the current (I_{off}) that would flow in the absence of a gate field, as in eqn. (3),

$$I_{on}/I_{off} = \mu_{FE}\ C_i\ V_G/2\mu_r\rho h \quad (3)$$

where μ_r and ρ are the mobility and density of residual charge and h is the height of the semiconducting layer.

As will be discussed below, useful on/off ratios ($>10^6$) can now be obtained from several organic semiconductors. While these materials have moderate mobilities, their intrinsic conductivities can be rendered vanishingly small through proper synthesis and purification techniques, leading to very low 'off' currents and lowering the denominator of the on/off ratio. Obtaining practically useful mobilities ($>0.1\ cm^2\ V^{-1}\ s^{-1}$) is not as facile,[6] as the intermolecular overlaps in most organic crystals are small and near-surface crystalline morphologies are imperfect. It would therefore be tempting to increase the 'on' current through chemical doping. This tactic has been extensively considered, and it was concluded that the off-conduction increases more rapidly with doping level than does mobility. Thus, the mobility of several different semiconductors approached $0.1\ cm^2\ V^{-1}\ s^{-1}$ at high dopant concentrations, but the conductivity became so high that the on/off ratio fell below 1.[7]

This key observation implies that molecular crystalline solids can be expected to be superior to polymeric semiconductors in TFTs. While much early TFT work was performed on conducting polymers such as polythiophene,[1,8] these materials are doped almost by definition, and probably cannot be purified to the same degree as discrete molecular compounds. While the polymer mobilities may have been respectable, largely because of the doping, the on/off ratios were not utilizable. However, from a processing standpoint, polymeric materials are still advantageous in that inexpensive condensed-phase deposition techniques are available that would avoid the high vacuum steps associated with the present use of molecular solid semiconductors, and thus remain attractive for further study.

Unsubstituted thiophene oligomers

The introduction of molecular crystals as TFT semiconductors may be credited to F. Garnier and his collaborators at CNRS, who first demonstrated devices with significant mobilities, on/off ratios and saturation behaviour using oligomeric thiophenes, chiefly the unsubstituted hexamer. The characteristics of such an early device are shown in Fig. 4. The preponderance of subsequent data on organic TFTs has also been obtained using α-sexithiophene (α-6T) as the semiconductor, so it is appropriate to probe the relevant chemistry, morphology and device physics of this compound in some detail.

There are three principal ways to synthesize α-6T from the commercially available terthiophene (α-3T), as shown in Scheme 1. Neutral α-3T may be oxidatively dimerized by ferric chloride in a nonpolar aromatic solvent, by a method described in a European Patent Application.[9] The chief advantage of this method lies in the convenience of the reaction conditions. The disadvantages are the undesirably large quantity of iron retained in the crude solid product and the finite probability of bond formation at carbons other than the terminal ones. Cleaner products are obtained when the α-3T starting material is first deprotonated with butyllithium or another strong lithium base, and then oxidized with copper(II) chloride.[10] This is probably the most widely employed method, and avoids the possibility of nonselective coupling. However, a minor side reaction occurs which places chloro groups at terminal carbons of the α-6T product.[11] Despite the low concentration of this contaminant, it is difficult or impossible to remove and could disrupt the solid state structure of films made from the product. Therefore, a third method was developed where the oxidizing

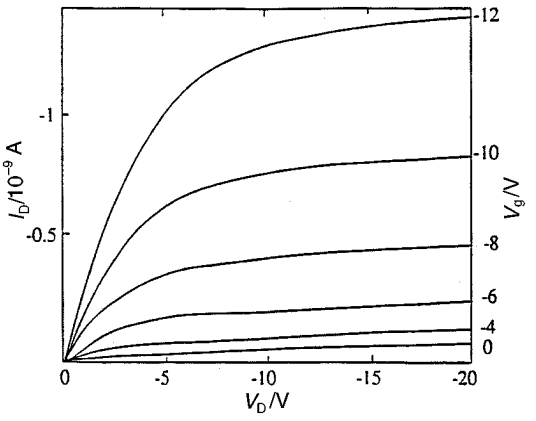

Fig. 4 Current–voltage plots for an early α-6T TFT [ref. 24(*a*)], with kind permission from Elsevier Science S.A., P.O. Box 564, 1001 Lausanne, Switzerland

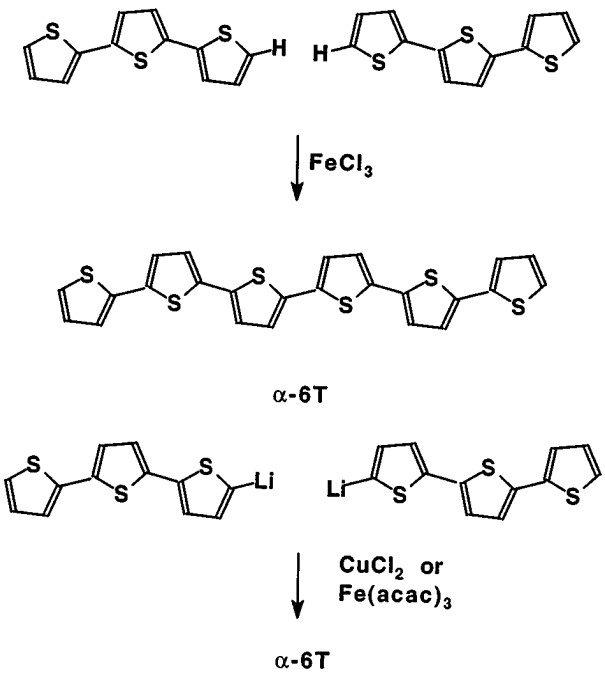

Scheme 1

agent for the lithiated α-3T is ferric acetylacetonate.[11,12] Besides again avoiding undesired regiochemistry, no terminally substituted α-6T products are detected even in crude products prepared this way.

The isolation of a suitable crude product is only the first step towards obtaining device-grade α-6T. It is also necessary to thoroughly triturate the crude product to remove small organic and inorganic impurities, and then recrystallize and sublime the product under inert atmosphere and vacuum, respectively, before reliable device characterization can be attempted. Establishment of this protocol was a key step in determining reliable and encouraging performance parameters for α-6T in TFTs.[11] These principles have also enabled high mobilities and on/off ratios to be observed in a variety of other compounds, as will be described later. The value of ultrapurification to organic device performance had already been well delineated for other classes of devices.[6,13]

α-6T Can be deposited in thin film form with a variety of morphologies. The deposition temperature, evaporation rate and functionality of the substrate all influence the grain size and molecular orientation of the films.[14] At room temperature and slow to moderate deposition rates (<5 Å s^{-1}) on polar surfaces, grain sizes on the order of 100 nm are obtained, with a preference for flat platelets containing molecules nearly perpendicular to the substrate, although some parallel molecular orientation also occurs. The molecular layer spacing is 23–24 Å, close to the molecular length. Very fast deposition or a substrate temperature of 77 K produces smaller grains, molecules parallel to the substrate and slightly larger layer spacing. On the other hand, a much higher substrate temperature of 260 °C results in exclusive perpendicular molecular orientation observable by X-ray and electron diffraction, UV–VIS dichroism and conductivity anisotropy. Elongated crystallites and new polymorphs are also observed, some of which may be mesophases,[15] with layer spacings distinct from those observed after room temperature deposition. The highest hole mobilities are observed with high temperature depositions because of the favourable morphology and because of the additional purification that occurs during film growth. Rapid thermal annealing or melt growth of the films leads to much larger crystalline domains, several micrometers in size, but with extensive fractures that limit the overall hole mobility.[16]

The single crystal structure of α-6T, and indeed, any of the unsubstituted oligomers higher than α-3T, has proved elusive until very recently. The structure of the trimer was determined in 1989, and was found to be nearly flat, with torsional angles of 6–9°.[17] The tetramer with terminal methyl groups was found to adopt a herringbone packing motif with a substantial tilt of the molecules with respect to the long unit cell axis.[18] This type of structure is common to many conjugated organics and will be seen to be a harbinger of the α-6T structure in many respects. The torsional angles between thiophene rings in the dimethyl α-4T are between 3 and 4°.

Several higher oligomer structures with internal alkyl and alkylthio substituents have been crystallographically determined.[19] Distortions imparted by the substituents include larger torsional angles, rotational disorder and poor intermolecular overlap. While certainly providing valuable insight, especially at the single molecule level, these compounds are not close models for the superstructures of the high oligomers. Crystalline polythiophene has been examined by X-ray diffraction, and the herringbone structure, chain planarity and alternating disposition of the thiophene rings have been established therein.[20] These structural features might therefore be reasonably predicted for unsubstituted high oligomers such as α-6T.

Crystal structures of α-6T were at last described in 1995.[21] Carefully controlled, solventless growth procedures were used to obtain the crystal specimens. Surprisingly, two different structures were found. They share the flat single molecule structure, monoclinic unit cell and herringbone packing common to several of the analogues described above. However, they differ in the position, density and orientation of the molecules with respect to the unit cell axes. For the so-called 'high temperature' polymorph,[21b] shown in Fig. 5, the energy band dispersions were calculated along the three principal axes of the reciprocal lattice. Significant dispersions were found along two of the axes, where 'sideways' carbon–sulfur contacts near the van der Waals distance occur. From this calculation, it could be inferred that high mobilities would be observed in those two dimensions. Furthermore, X-ray diffraction shows that the related oligomers α-4T and α-8T pack in arrangements virtually identical to that of α-6T, both as bulk solids and with respect to substrate surfaces in thin film form, a prediction borne out by a very recent single crystal study.[22]

In the initial demonstration of organic TFTs,[23] it appeared that the hexamer represented the minimum length for substantial mobility among the oligothiophenes. The value obtained, on the order of 10^{-4} cm^2 V^{-1} s^{-1}, was similar to that previously observed in conjugated polymers, and was probably similarly dependent on doping and defect levels. Immediately subsequent work[24] indicated a strong dependence of mobility on the nature of the gate dielectric and further emphasized the hexamer as the optimal length. A thorough and understandable model was also presented to account for the behaviour of the

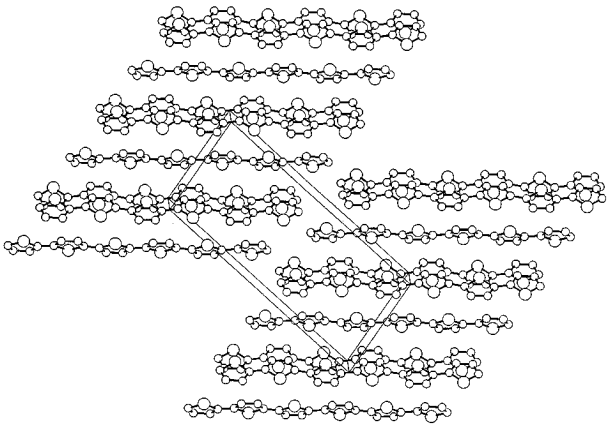

Fig. 5 Herringbone packing motif and unit cell definition for the 'high temperature' phase of α-6T

devices, using the standard equations and also including the role of traps in determining the threshold voltage, above which the most significant gate-induced currents are observed. Finally, it was predicted that improved purification of the α-6T would lead to higher mobilities, along with a preliminary verification.

Indeed, it was later rigorously shown that improved refinement methods described above lead not only to higher mobilities, well above 0.01 $cm^2\ V^{-1}\ s^{-1}$, but also greatly reduced off-currents, so that the on/off ratio reaches one million and the semiconductor could be described as intrinsic.[11,25] Characteristics of such a device are shown in Fig. 6, where it may be noted that the current is at the detection limit at zero gate voltage, without the need for extra 'depletion' voltage. Improvements were also noted for α-4T and α-8T; in fact, the latter compound had mobility comparable to the hexamer, and α-4T was noteworthy for its extremely low off-current.[11] A careful analysis of the film thickness and channel length dependencies of the field-induced currents showed that the channel in α-6T is confined to an extremely thin region, perhaps as thin as 50 Å, near the dielectric.[25] A 'two-dimensional' solid is formed, not primarily because of the morphology, which does happen to be anisotropic, but mainly because of the potential well that forms near the dielectric interface and that extends only one to a few monolayers outward. A hint that the mobility could be further enhanced was derived from a positive mobility dependence on source–drain voltage above 0.1 MV cm^{-1}. These more detailed observations were incorporated into a more comprehensive model that also takes into account circuit elements arising from the unpatterned deposition of the semiconductor and features of the external circuit.[26] It has also been shown that the temperature dependence of the α-6T mobility from 4 K to ambient is nonmonotonic, with a minimum near 45 K.[27] This behaviour is consistent with Holstein's theory for small polaron motion, and data can be fitted by the same set of parameters on both sides of the minimum, except at the very lowest temperatures, as shown in Fig. 7. Since these parameters (polaron binding energy and carrier–lattice coupling) are associated with bulk material properties, it is unlikely that the microscopic mobility is limited by grain boundaries, and likely that the mobility can be enhanced by uncovering materials for which these parameters are more favourable. There are also indications that crystalline disorder affects the polaron binding energies. Most recently, using a different approach, an enhanced mobility of $>0.07\ cm^2\ V^{-1}\ s^{-1}$ has been observed by constructing transistors from single crystals of α-6T mounted on the gate dielectrics with source and drain electrodes deposited on the opposite face of the crystal.[28] It is not yet known whether the single crystal is in a phase with more favourable (lower) values of the Holstein parameters, or whether the high mobility is due to the avoidance of gross cracks and contact delamination.

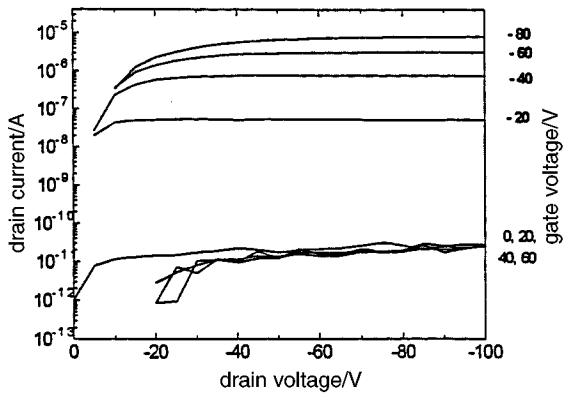

Fig. 6 Current–voltage plots for an 'intrinsic' (dopant-free) α-6T TFT. Note that the current scale is logarithmic.

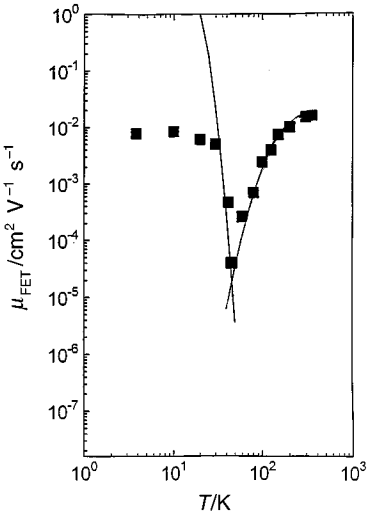

Fig. 7 Temperature dependence of the mobility of α-6T. The squares are experimental data and the solid curves are fits to the Holstein theory.

Unsubstituted oligothiophenes have been applied to electronic devices as Langmuir–Blodgett films[29] as well as by evaporation. Besides TFTs, Schottky diodes[30] and active optical devices[31] have been fabricated. The interplay of optical and electronic effects in thiophene oligomers has recently been investigated.[32]

End-substituted thiophene hexamers

The placing of substituents on oligothiophenes is an attractive strategy because of the possibility of electronic tuning, increased processing options and control of the film morphology. As discussed above, substitution anywhere other than at the 4- or 5-carbons of the terminal rings leads to severe distortions of the conformation and intermolecular overlap and would probably be unproductive. Benefits have in fact been realized by the 5-alkyl substitution of α-6T.[33,34] Two synthetic strategies have been developed for accomplishing this, outlined in Scheme 2. In the first, commercially available alkylthiophenes are appended to 5-bromobithiophene *via* alkylthienylzinc reagents to form alkylterthiophenes, which are

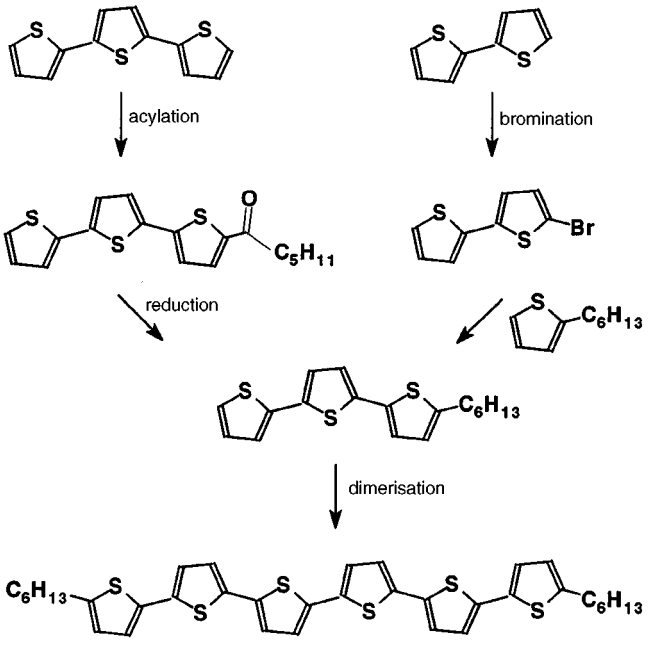

Scheme 2

then lithiated and dimerized.[33] A second route begins with the acylation of α-3T followed by deoxygenation of the product.[34] The first route avoids the limited yield associated with the acylation step, but requires careful chromatography. The second route employs simpler chromatography because of the polarity contrast of the acylterthiophene intermediate and provides greater choice over the nature of the eventual alkyl substituent. Unlike the case of the unsubstituted derivatives, $CuCl_2$ is a suitable coupling reagent for the alkylterthienyllithiums because no chlorinated hexathienyls can form, and it is advantageous to utilize the relatively high reactivity of $CuCl_2$ to intercept the lithiated compounds before they can isomerize to (1-lithioalkyl) compounds.

Dihexylated α-6T forms a much smoother, orientationally homogeneous film than does the unsubstituted parent.[33] The ordered domains are larger and the hexathienyl cores are directed at a slight but consistent tilt angle relative to the substrate normal. The influence of the alkyl chains on the morphology is manifest in the three melting transitions, evidence of mesophases, observed with this compound.[34] The mobility is 0.05 $cm^2\ V^{-1}\ s^{-1}$, higher than typically achieved without substitution, and less prone to diminution by contaminants than that of α-6T. The dihexyl compound has been used in devices where organic conductive leads were printed on plastic substrates.[35] Use of dodecyl substituents on α-6T yields a material with mobility comparable to the parent, even though the proportional volumes of the active moieties and inert substituents are comparable.[36] The melting points are further lowered and the solubility is increased. It has been demonstrated that oligothiophenes with fused tetrahydrobenzo endcaps may be deposited with extremely low conductivities, useful for low off-currents, although these films are susceptible to oxygen doping.[37]

In an attempt to lower the barrier to hole injection, α-6T with hexylthio substituents was synthesized.[34] Unfortunately, doping and decomposition levels were too high for this material to be considered useful. Routes to additional α-6T derivatives with more elaborate substituents, including polyethers and electron withdrawing substituents such as formyl and cyano, have also been devised.[38]

Fused ring compounds

In trying to determine whether catenated thiophenes are essential to the construction of organic semiconductors, a compound with the thiophenes incorporated into fused benzodithiophene rings was prepared.[39] The synthesis is based on what was originally reported for that ring system, followed by ferric acetylacetonate coupling (Scheme 3). A mobility of 0.04 $cm^2\ V^{-1}\ s^{-1}$ was observed, despite fewer sulfurs, fewer

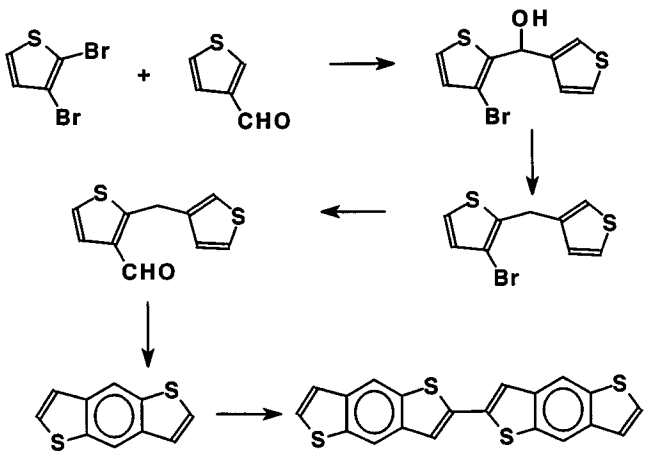

Scheme 3

total heavy atoms and a different linkage compared to α-6T. The melting point of this compound is very high, over 400 °C, and the morphology consists of smooth interconnected grains with perpendicular orientation. These favourable properties are best obtained when the substrate temperature is 100 °C. The conformation of the molecule would be expected to be flatter than that of α-6T.

At the same time, the semiconducting properties of pentacene[23] were revisited.[40] The mobility of pentacene turns out to be extremely sensitive to the deposition conditions. Variations in the deposition rate over 1–2 orders of magnitude and substrate temperature over just tens of degrees about ambient produces films ranging from 10^{-6} to 3×10^{-2} $cm^2\ V^{-1}\ s^{-1}$. This is due to the striking changes in morphology that accompany these variations. At the extremes of low temperature and/or low deposition rate, amorphous films are produced, while at more moderate deposition rates and slightly elevated temperatures, polycrystalline films reminiscent of thiophene oligomers are obtained. A novel liquid-phase deposition of a soluble pentacene Diels–Alder adduct followed by *in situ* thermal conversion to pentacene produced a mobility of 10^{-3} $cm^2\ V^{-1}\ s^{-1}$, and represents a first approach to higher-order devices including ring oscillators and logic gates made without high-vacuum deposition of the semiconductor.[2] The morphology of these latter films was considered to be amorphous.[40]

More recently, mobilities as high as 0.6 $cm^2\ V^{-1}\ s^{-1}$ were reported for pentacene deposited at elevated temperature using top contact geometry.[41] This is a breakthrough value for organic TFTs, similar to the hole mobility measured in highly purified organic single crystals such as naphthalene and anthracene using transient photoconductivity techniques,[6] and also approaches the electron mobility of amorphous silicon.[42] The exceptional performance of this form of pentacene has been traced to its forming large (1–10 micron) thin film single crystal domains, on the order of the device sizes.[43] Fig. 8 shows a comparison of the device characteristics and electron diffraction patterns of TFT films deposited at ambient temperature and 85 °C. The high temperature electron diffraction pattern shows single crystallinity, with the long molecular axes perpendicular to the substrate. The highest mobility is associated with this morphology.

Pentacene shares the flat ribbon shape common to the thiophene oligomers and the benzodithiophene dimer discussed above. However, its lack of heteratoms indicates that sulfurs are not essential for either favourable morphology or high mobility. It would still be an open question as to whether the ribbon shape is necessary. Some evidence to the contrary has been derived from phthalocyanines, which are planar but four-fold symmetric. Fair mobilities have been reported for phthalocyanine derivatives in highly conductive states.[7] More recent work has identified phthalocyanine derivatives which show mobility comparable to α-6T and edge-on morphologies in undoped, low conductivity states.[44] Thus, TFT films can conceivably be fabricated from compounds lacking sulfurs and high aspect ratios.

In the course of our own compound screening, we have considered p-type compounds such as biphenylenediamines[45] commonly used in organic light-emitting diodes and 5,7,12,14-tetrathiapentacene for TFTs. These compounds are not strictly planar and to date have not shown high TFT mobilities. Our present belief is that planarity is extremely important in designing high mobility p-type compounds.

n-Channel organic transistors

The range of organic compounds that transport predominantly electrons is much more limited than those which are effective hole transporters. The highest mobilities have been found with C_{60}-based TFTs:[46] 0.08 $cm^2\ V^{-1}\ s^{-1}$ for the neat material, and

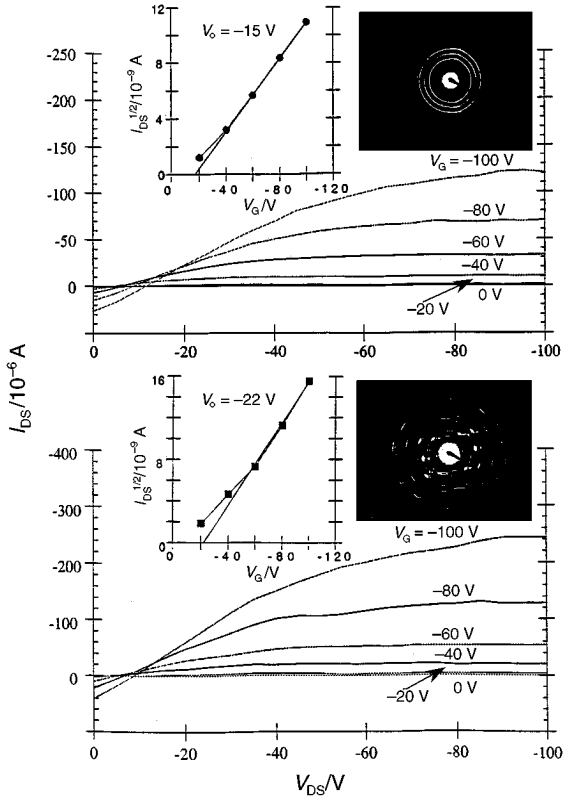

Fig. 8 Current–voltage plots for pentacene deposited on (*a*) ambient-temperature and (*b*) 85 °C (bottom figure) substrates. The insets are plots to determine the threshold voltages, and the electron diffractograms.

a factor of 3–4 higher for devices grown on substrates pre-treated with tetrakis(dimethylamino)ethylene. The characteristics are shown in Fig. 9; the signs of the gate voltage and drain current are opposite those for p-type devices. These devices are all much more sensitive to the atmosphere than are p-type devices, partly because of the chemical sensitivity of C_{60} itself, and partly because of the inherent oxygen sensitivity of electrons ('radical anions') in organic materials. Temperature- and field-effect mobility have also been measured for a C_{60}/C_{70} mixture containing about 10% C_{70}.[47]

Another class of electron carriers are the dyes based on perylenetetracarboxylic dianhyride (PTCDA) and its derivatives PTCDI and NTCDA.

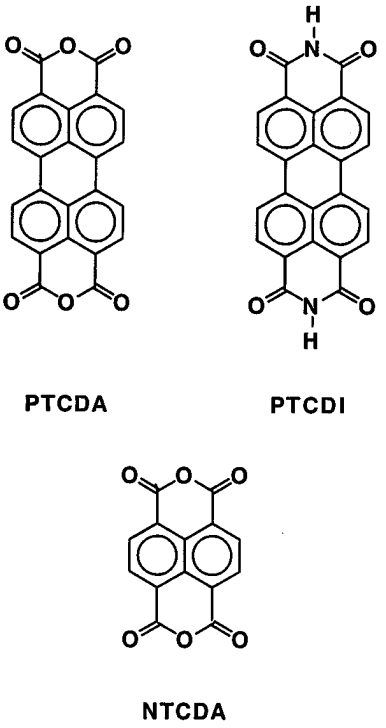

PTCDA has an electron mobility of 10^{-5} to 10^{-4} cm^2 V^{-1} s^{-1} in TFTs.[48] The low mobility is due in part to a morphology which has the molecules lying flat on the surface of the dielectric. Interestingly, PTCDA transports mainly holes in the molecular stacking direction, which happens to be perpendicular to the direction of transport in a TFT. Slightly lower mobilities are found with substituted and unsubstituted imides,[49] probably reflecting the expected lower electron affinities of the imides. On the other hand, NTCDA shows higher mobility than the more delocalized PTCDA.[50] Although all of these compounds are more stable than C_{60}, the devices again degrade rapidly with operation in air. This degradation is reversible, and the devices resume their normal operating characteristics when moisture is removed from the ambient. It is possible that higher apparent mobilities would arise from use of lower work function electrodes, compounds with improved morphologies or molecules with higher electron affinities. These routes are being explored. For example, tetracyanoquinodimethane has a very high electron affinity, but only a fair mobility in a highly doped state.[7]

One higher order effect that has been demonstrated using n-type semiconductors is related to complementary circuit fabrication. Heterostructure field effect transistors displaying distinguishable n- and p-type behaviour in the same devices have been made from thiophene hexamers as p-type materials and C_{60}, or PTCDA as n-type.[51] This double polarity behaviour is shown for α-6T/C_{60} in Fig. 10. The function of such a device could be determined in a circuit by the sign of the gate voltage applied to it. Circuits containing complementary transistors are important where low power dissipation is a major consideration.

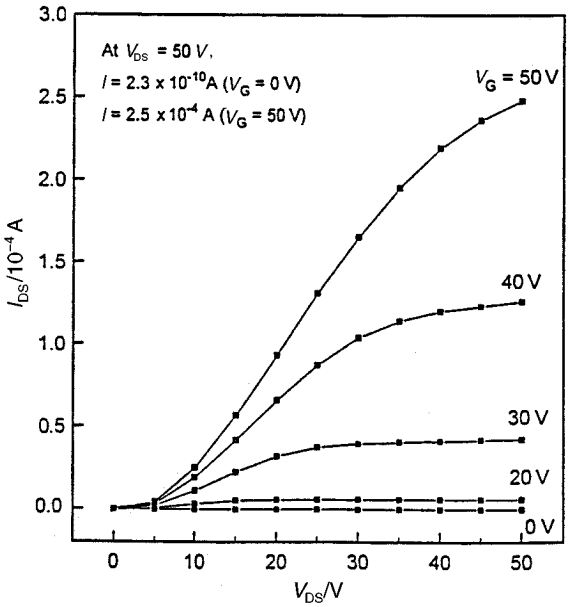

Fig. 9 Current–voltage plots for an n-channel, C_{60}-based TFT

Summary and outlook

The range of organic molecules displaying substantial semiconducting action in TFTs has been expanded to include various shapes and constitutions. Several approaches to high hole mobility have been uncovered, and electron mobility may also now be seriously considered. A major ongoing challenge is to produce the highest mobility morphologies without the high

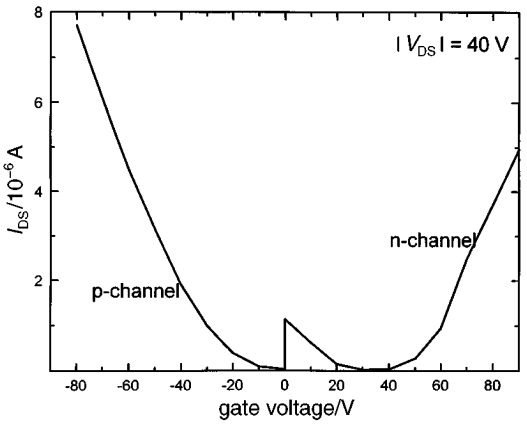

Fig. 10 Current flow at constant absolute source–drain voltage in a single α-6T/C_{60} heterostructure TFT as a function of sign and magnitude of the gate voltage. Substantial currents for both negative drain and gate (p-channel) and positive drain and gate (n-channel) operation are observed.

vacuum deposition procedure, to achieve the most valuable gains in process efficiency. Once devices are fabricated in this manner, their packaging and reliability will be an additional serious concern. The issues of process sequence and long term stability should evolve as the main foci of future organic TFT investigations.

I am grateful to my colleagues, named in many of the references, for a most productive collaboration. I particularly would like to thank A. Dodabalapur and J. Laquindanum for helpful suggestions regarding this manuscript. Finally, I would like to acknowledge Drs T. Jackson, Yen Wei and D. Dimitrikopoulos for sharing results prior to publication.

References

1 (*a*) H. Stubb, E. Punkka and J. Paloheimo, *Mater. Sci. Eng*., 1993, **10**, 85; (*b*) C. P. Jarrett, R. H. Friend, A. R. Brown and D. M. de Leeuw, *J. Appl. Phys*., 1995, **77**, 6289.
2 A. R. Brown, A. Pomp, C. M. Hart and D. M. de Leeuw, *Science*, 1995, **270**, 972.
3 A. K-Y. Jen, C. Y-C. Lee, L. R. Dalton, M. F. Rubner, G. E. Wnek and L. Y. Chiang, *Mater. Res. Soc. Symp. Proc*., 1995, **413**.
4 Y. Y. Lin, D. J. Gundlach and T. N. Jackson, *Mater. Res. Soc. Symp. Proc*., 1995, **413**, 413.
5 A. Dodabalapur, L. Torsi and H. E. Katz, *Adv. Mater*., in the press.
6 W. Warta, R. Stehle and N. Karl, *Appl. Phys. A*, 1985, **36**, 163.
7 A. R. Brown, D. M. de Leeuw, E. E. Havinga and A. Pomp, *Synth. Met*., 1994, **68**, 65.
8 A. Tsumura, H. Koezuka and T. Ando, *Appl. Phys. Lett*., 1986, **49**, 1210.
9 (*a*) D. Fichou, G. G. Horowitz and F. Garnier, *Eur. Pat. Appl.* EP 402,269, 1990; *FR Appl.* 89/7,610, 1989; (*b*) T. Kurata, K. Hamano, S. Kubota and H. Koezuka, *Organic Thin Films for Photonic Applications*, Toronto, 1993, p. 186. (*c*) M. S. A. Abdou, X. Lu, Z. W. Xie, F. Orfino, M. J. Deen and S. Holdcroft, *Chem. Mater*., 1995, **7**, 631.
10 (*a*) J. Kagan and S. K. Arora, *Heterocycles*, 1983, **20**, 1937; (*b*) M-T. Zhao, B. P. Singh and P. N. Prasad, *J. Chem. Phys*., 1988, **89**, 5535.
11 H. E. Katz, L. Torsi and A. Dodabalapur, *Chem. Mater*., 1995, **7**, 2235.
12 (*a*) H. E. Katz and D. J. Cram, *J. Am. Chem. Soc*., 1984, **106**, 4977; (*b*) M. J. Marsella and T. M. Swager, *J. Am. Chem. Soc*., 1993, **115**, 12214.
13 F. F. So, S. R. Forrest, Y. Q. Shi and W. H. Steier, *Appl. Phys. Lett*., 1990, **56**, 674.
14 (*a*) B. Servet, G. Horowitz, S. Ries, O. Lagorsse, P. Alnot, A. Yassar, F. Deloffre, P. Srivastava, R. Hajlaoui, P. Lang and F. Garnier, *Chem. Mater*., 1994, **6**, 1809; (*b*) A. J. Lovinger, D. D. Davis, R. Ruel, L. Torsi, A. Dodabalapur and H. E. Katz, *J. Mater. Res*., 1995, **10**, 2958.
15 S. Destri, M. Mascherpa and W. Porzio, *Adv. Mater*., 1993, **5**, 43.
16 (*a*) L. Torsi, A. Dodabalapur, A. J. Lovinger, H. E. Katz, R. Ruel, D. D. Davis and K. W. Baldwin, *Chem. Mater*., 1995, **7**, 2247; (*b*) A. J. Lovinger, D. D. Davis, A. Dodabalapur, H. E. Katz and L. Torsi, *Macromolecules*, 1996, **29**, 4952.
17 F. Van Bolhuis, H. Wynberg, E. E. Havinga, E. W. Meijer and E. G. J. Staring, *Synth. Met*., 1989, **30**, 381.
18 (*a*) S. Hotta and K. Waragai, *J. Mater. Chem*., 1991, **1**, 835; (*b*) S. Hotta and K. Waragai, *Adv. Mater*., 1993, **5**, 896.
19 (*a*) G. Barbarella, M. Zambianchi, R. Di Toro, M. Colonna, L. Antolini and A. Bongini, *Adv. Mater*., 1996, **8**, 327; (*b*) J-H. Liao, M. Benz, E. LeGoff and M. G. Kanatzidis, *Adv. Mater*., 1994, **6**, 135; (*c*) J. K. Herrema, J. Wildeman, F. van Bolhuis and G. Hadziioannou, *Synth. Met*., 1993, **60**, 239.
20 (*a*) Z. Mo, K-B. Lee, Y. B. Moon, M. Kobayashi, A. J. Heeger and F. Wudl, *Macromolecules*, 1985, **18**, 1972; (*b*) W. Porzio, S. Destri, M. Mascherpa, S. Rossini and S. Brückner, *Synth. Met*., 1993, **55–57**, 408.
21 (*a*) G. Horowitz, B. Bachet, A. Yassar, P. Lang, F. Demanze, J-L. Fave and F. Garnier, *Chem. Mater*., 1995, **7**, 1337; (*b*) T. Siegrist, R. M. Fleming, R. C. Haddon, R. A. Laudise, A. J. Lovinger, H. E. Katz, P. M. Bridenbaugh and D. D. Davis, *J. Mater. Res*., 1995, **10**, 2170.
22 A. J. Lovinger, D. D. Davis, A. Dodabalapur and H. E. Katz, unpublished results; D. Fichou, B. Bachet, F. Demanze, I. Billy, G. Horowitz and F. Garnier, *Adv. Mater*., 1996, **8**, 500.
23 G. Horowitz, D. Fichou, X. Peng and F. Garnier, *Synth. Met*., 1991, **41–43**, 1127.
24 (*a*)F. Garnier, G. Horowitz, X. Z. Peng and D. Fichou, *Synth. Met*., 1991, **45**, 163; (*b*) G. Horowitz and P. Delannoy, *J. Chim. Phys*., 1992, **89**, 1037.
25 A. Dodabalapur, L. Torsi and H. E. Katz, *Science*, 1995, **268**, 270.
26 L. Torsi, A. Dodabalapur and H. E. Katz, *J. Appl. Phys*., 1995, **78**, 1088.
27 L. Torsi, A. Dodabalapur, L. J. Rothberg, A. W. P. Fung and H. E. Katz, *Science*, 1996, **272**, 1462.
28 G. Horowitz, F. Garnier, A. Yassar, R. Hajlaoui and F. Kouki, *Adv. Mater*., 1996, **8**, 52.
29 (*a*) S. Tasaka, H. E. Katz, R. S. Hutton, J. Orenstein, G. H. Fredrickson and T. T. Wang, *Synth. Met*., 1986, **16**, 17; (*b*) J. Paloheimo, P. Kuivalainen, H. Stubb, E. Vuorimaa and P. Yli-Lahti, *Appl. Phys. Lett*., 1990, **56**, 1157.
30 (*a*) D. Fichou, G. Horowitz, Y. Nishikitani, J. Roncali and F. Garnier, *Synth. Met*., 1989, **28**, C729; (*b*) D. Fichou, G. Horowitz, Y. Nishikitani and F. Garnier, *Chemtronics*, 1988, **3**, 176; (*c*) M. Ahlskog, J. Paloheimo, H. Stubb and A. Assadi, *Synth. Met*., 1994, **65**, 77.
31 (*a*) H. Knoblock, D. Fichou, W. Knoll and H. Sasabe, *Adv. Mater*., 1993, **5**, 570; (*b*) H. Thienpont, G. L. J. A. Rikken, E. W. Meijer, W. ten Hoeve and H. Wynberg, *Phys. Rev. Lett*., 1990, **65**, 2141; (*c*) D. Fichou, J-M. Nunzi, F. Charra and N. Pfeffer, *Adv. Mater*., 1994, **6**, 64.
32 D. Fichou and F. Charra, *Synth. Met*., 1996, **76**, 11.
33 F. Garnier, A. Yassar, R. Hajlaoui, G. Horowitz, F. Deloffre, B. Servet, S. Ries and P. Alnot, *J. Am. Chem. Soc*., 1993, **115**, 8716.
34 H. E. Katz, A. Dodabalapur, L. Torsi and D. Elder, *Chem. Mater*., 1995, **7**, 2238.
35 F. Garnier, R. Hajlaoui, A. Yasser and P. Srivastava, *Science*, 1994, **265**, 684.
36 J. Laquindanum and H. E. Katz, unpublished results.
37 C. Väterlein, B. Ziegler, W. Gebauer, H. Neureiter, M. Stoldt, M. S. Wever, P. Bäuerle, M. Sokolowski, D. D. C. Bradley and E. Umbach, *Synth. Met*., 1996, **76**, 133.
38 Y. Wei, Y. Yang and J-M. Yeh, *Chem. Mater*., 1996, **8**, 2659.
39 J. Laquindanum, H. E. Katz, A. Dodabalapur and A. J. Lovinger, *Adv. Mater*., in the press.
40 C. D. Dimitrakopoulos, A. R. Brown and A. Pomp, *J. Appl. Phys*., 1996, **80**, 2501.
41 Y. Y. Lin, D. J. Gundlach and T. N. Jackson, *Device Research Conference*, Santa Barbara, 1996, p. 175.
42 *Amorphous and Microcrystalline Semiconductor Devices: Optoelectronic Devices*, ed. J. Kanicki, Artech House, Boston, 1991.
43 J. Laquindanum, H. E. Katz, A. J. Lovinger and A. Dodabalapur, *Chem. Mater*., 1996, **8**, 2542.
44 Z. Bao, A. Dodabalapur and A. J. Lovinger, *Appl. Phys. Lett*., 1996, **69**, 3066.
45 P. M. Borsenberger, W. T. Gruenbaum, L. J. Sorriero and N. Zumbulyadis, *Jpn. J. Appl. Phys*., 1995, **34**, 1597.
46 R. C. Haddon, A. S. Perel, R. C. Morris, T. T. M. Palstra, A. F. Hebard and R. M. Fleming, *Appl. Phys. Lett*., 1995, **67**, 121.

47 J. Paloheimo, H. Isotalo, J. Kastner and H. Kuzmany, *Synth. Met*., 1993, **55–57**, 3185.
48 J. R. Ostrick, A. Dodabalapur, L. Torsi, A. J. Lovinger, E. W. Kwock, T. M. Miller, M. Galvin and H. E. Katz, unpublished results.
49 G. Horowitz, F. Kouki, P. Spearman, D. Fichou, C. Nogues, X. Pan and F. Garnier, *Adv. Mater*., 1996, **8**, 242.
50 J. Laquindanum, H. E. Katz, A. Dodabalapur and A. J. Lovinger, *J. Am. Chem. Soc*., 1996, **118**, 11 331.
51 A. Dodabalapur, H. E. Katz, L. Torsi and R. C. Haddon, *Science*, 1995, **269**, 1560.

Paper 6/05274F; *Received* 29*th July*, 1996